Numerical Analysis of Nonminimum Phase Zero for Nonuniform Link Design

Douglas L. Girvin and Wayne J. Book

George W. Woodruff School of Mechanical Engineering
Georgia Institute of Technology
Atlanta, GA 30332

ABSTRACT

As the demand for light-weight robots that can operate in a large workspace increases, the structural flexibility of the links becomes more of an issue in control . When the objective is to accurately position the tip while the robot is actuated at the base, the system is nonminimum phase. One important characteristic of nonminimum phase systems is system zeros in the right half of the Laplace plane. The ability to pick the location of these nonminimum phase zeros would give the designer a new freedom similar to pole placement.

This research targets a single-link manipulator operating in the horizontal plane and modeled as a Euler-Bernoulli beam with pinned-free end conditions. Using transfer matrix theory, one can consider link designs that have variable cross-sections along the length of the beam. A FORTRAN program was developed to determine the location of poles and zeros given the system model. The program was used to confirm previous research on nonminimum phase systems, and develop a relationship for designing linearly tapered links. The method allows the designer to choose the location of the first pole and zero and then defines the appropriate taper to match the desired locations. With the pole and zero location fixed, the designer can independently change the link's moment of inertia about its axis of rotation by adjusting the height of the beam. These results can be applied to inverse dynamic algorithms currently under development at Georgia Tech and elsewhere.

INTRODUCTION

Controller design for collocated systems has been heavily researched and is well understood compared to controller design for noncollocated systems. In noncollocated systems, uncertainties from model inaccuracies and modal truncation present fundamental problems with system performance and stability [18]. The fundamental difference between collocated and noncollocated systems is the presence of these RHP zeros. To advance controller design for noncollocated systems, research needs to be conducted into the factors that affect the location of these RHP zeros. This research targets the relationship between RHP zeros and structural design.

Although research on RHP zeros is limited, there has been some notable research done in the past. In 1988, Nebot and Brubaker [13] experimented with a single-link flexible manipulator. In 1989, Spector and Flashner [19] investigated the sensitivity effects of structural models for noncollocated control systems. In 1990, Spector and Flashner [18] again studied modeling and design implications pertinent to noncollocated control. Also in 1990, Park and Asada [15],[14] investigated a minimum phase flexible arm with a torque actuation mechanism. In 1991, Park, Asada, and Rai [1] expanded their previous work on a minimum phase flexible arm with a torque transmission device.

The underlying issue in noncollocated control is how to deal with the RHP zeros in the control algorithm. A major step in solving the problem is understanding what design parameters can be used to change the location of these RHP zeros. This research targets the relationship between RHP zero location and structural design. Specifically, how do changes in the shape of the structure (link) affect the location of these zeros?

Traditionally links are designed with uniform properties along the length because analytic solutions to this problem exist. A link with variable cross-section cannot be solved analytically, but with aid of a computer a numerical approximation can be found. The key to an accurate numerical solution is a good model of the system.

The research presented in this paper models a single-link flexible rotary manipulator as a pinned-free beam. Transfer matrix theory was used to generate a beam with variable cross-section. FORTRAN code was written to generate the model and evaluate the system for the location of RHP zeros. The program was used to examine the relationship between link shape and RHP zero location. This

relationship can be directly applied to controller design using the inverse dynamics approach researched at Georgia Tech and elsewhere.

TRANSFER MATRIX THEORY

Transfer matrices describe the interaction between two serially connected elements. These elements can be beams, springs, rotary joints, or many others. In 1979 Book, Majette, and Ma [6] and Book [4] (1974) used transfer matrices to develop an analysis package for flexible manipulators. They used transfer matrices to serially connect different types of elements to model the desired manipulator. Of interest in this paper is how to connect similar types of transfer matrices (beam elements) to model a beam with different cross-sectional area. Pestel and Leckie [16] provide an in depth discussion of transfer matrix derivations and applications.

Transfer matrices can be mathematically expressed by Equation 3.1. The state vector u_i is given by the state vector u_{i-1} multiplied by the transfer matrix B.

$$u_i = [B_i]u_{i-1} \qquad (3.1)$$

When elements are connected serially, the states at the interface of two elements must be equal. By ordered multiplication of the transfer matrices, intermediate states can be eliminated to determine the transfer matrix for the overall system.

The concept of state vector in transfer matrix theory is not to be confused with the state space form of modern control theory. The state equation in modern control theory relates the states of the system as a function of time. In transfer matrix theory the state equation relates the states at various points along the serial chain of elements. The independent variable in a transfer matrix is the Laplace or Fourier variable with units of frequency, not time. The elements of the matrix B depend on the frequency variable and therefore the states will change as the system frequency changes. The transfer matrix B essentially contains the (Laplace or Fourier) transformed dynamic equations of motion that govern the element in analytic form. Therefore, analytical solution of the transfer matrix alone does not involve numerical approximations to the partial differential equation modelling the beam. This is desirable since numerical approximations introduce error into the solution.

A single-link manipulator as pictured in Figure 3.1 can be thought of as a beam with torque applied at one end and free at the other end. There are several steps to determine the RHP zeros and imaginary poles of this system. First, develop a model for the beam. Second, determine the appropriate boundary conditions. Third, determine the system input and output. Fourth, solve for the system zeros. The following sections will discuss each of these steps in more detail.

A link with nonuniform cross-sections can be modeled as a series of discrete elements. While the shape of these elements is similar, the size can vary to allow for changes in cross-section. The appropriate element to model

a flexible link is an Euler-Bernoulli beam element. The Euler-Bernoulli model neglects the effects of rotary inertia and shear deformation in the element. [11]. This assumption is generally valid for modeling beams whose length is roughly ten times the thickness. Flexible manipulators have long, slender links which are appropriately modeled under the Euler-Bernoulli assumption.

Transfer matrices are derived from the equation of motion for a given element. For a uniform Euler-Bernoulli beam element, the equation of motion transformed to the frequency domain has the form:

$$\frac{d^4 w(x,\omega)}{dx^4} = \frac{\mu\omega^2}{EI} w(x,\omega)$$

where,

μ = mass density per unit length

ω = frequency in radians/second

E = Young's modulus

I = Cross sectional area moment of inertia

Notice the equation is fourth order thus requiring four states to describe the solution in transfer matrix form. The state vector for the Euler-Bernoulli element is:

$$u = \begin{bmatrix} -w \\ \psi \\ M \\ V \end{bmatrix} = \begin{bmatrix} displacement \\ slope \\ moment \\ shear\ force \end{bmatrix} \qquad (3.3)$$

The first two elements of the state vector are displacements (w and ψ) while the last two elements are forces (V and M). This arrangement of states is characteristic of transfer matrix theory.

An analytic solution to Equation 3.2 can be found when the element has uniform properties (ie. constant cross-section, mass density, and stiffness). Equation 3.4 gives the transfer matrix for a uniform Euler-Bernoulli element. Each element of Equation 3.4 is a function of frequency and must be reevaluated as the frequency of interest changes.

$$TM = \begin{bmatrix} C_0 & lC_1 & aC_2 & alC_3 \\ \dfrac{\beta^4 C_3}{l} & C_0 & \dfrac{aC_1}{l} & aC_2 \\ \dfrac{\beta^4 C_2}{a} & \dfrac{\beta^4 lC_3}{a} & C_0 & lC_1 \\ \dfrac{\beta^4 C_1}{al} & \dfrac{\beta^4 C_2}{a} & \dfrac{\beta^4 C_3}{l} & C_0 \end{bmatrix} \qquad (3.4)$$

2

where,

$$C_0 = \frac{1}{2}(\cosh\beta + \cos\beta) \qquad (3.5)$$

$$C_1 = \frac{1}{2\beta}(\sinh\beta + \sin\beta) \qquad (3.6)$$

$$C_2 = \frac{1}{2\beta^2}(\cosh\beta - \cos\beta) \qquad (3.7)$$

$$C_3 = \frac{1}{2\beta^3}(\sinh\beta - \sin\beta) \qquad (3.8)$$

and

$$\beta^4 = \frac{\omega^2 l^4 \mu}{EI} \quad (3.9) \qquad\qquad a = \frac{l^2}{EI} \quad (3.10)$$

With the transfer matrix for the fundamental beam elements, one can combine these elements serially to generate a model for the link. Figure 3.3 illustrates how a simple model can be constructed for a tapered beam. Although only two elements are considered here, more elements can be added to better approximate the shape of the link. Since the states at interface u_1 are the same for both elements, u_1 can be eliminated to obtain an overall transfer matrix for the beam:

$$u_2 = [B_2][B_1]u_0 \qquad (3.13)$$

Eliminating one state simply illustrates the point that this multiplication can be carried out to eliminate all intermediate states in a model with more elements.

As previously mentioned, transfer matrices themselves are not numerical approximations. The transfer matrix for a Euler-Bernoulli beam contains the analytic solution for a uniform beam element. It is not an assumed modes solution. The approximation made in using transfer matrix theory involves the modeling of the beam and solution of the equations. To generate the model of a link with variable cross-section, the size of the elements must vary. The interface of two different size elements will be discontinuous. In Figure 3.3, interface 1 is discontinuous between elements A and B. These discontinuities are the major approximation when using transfer matrices to model a beam. This approximation can be minimized by using more elements to model a nonuniform beam. As more elements are added to the model, the discontinuities between elements will decrease thus reducing the effects of this approximation on the results.

Transfer matrix theory as used to represent a variable cross section is similar to Finite Element Analysis (FEA). In FEA, first the system must be discretized. Then an appropriate interpolation function must be selected to

describe each element (ie. element stiffness). Next the system matrices must be assembled to produce a set of linear algebraic equations. Finally the linear equations are solved to get an approximate solution to the system under consideration. These boundary conditions are applied to the overall transfer matrix for the system and the appropriate state variables are set to zero.

$$\begin{bmatrix} -w \\ \psi \\ 0 \\ 0 \end{bmatrix}_{x=L} = \begin{bmatrix} B_{11} & \cdots & B_{14} \\ \vdots & \ddots & \vdots \\ B_{41} & \cdots & B_{44} \end{bmatrix} \begin{bmatrix} 0 \\ \psi \\ 0 \\ V \end{bmatrix}_{x=0} \qquad (3.14)$$

Since this research targets the location of RHP zeros the system output is tip position, and the system input is joint torque. Considering the system input and output, the overall system transfer matrix will have the form:

$$\begin{bmatrix} -w \\ \psi \\ 0 \\ 0 \end{bmatrix}_{x=L} = \begin{bmatrix} B_{11} & \cdots & B_{14} \\ \vdots & \ddots & \vdots \\ B_{41} & \cdots & B_{44} \end{bmatrix} \begin{bmatrix} 0 \\ \psi \\ \tau \\ V \end{bmatrix}_{x=0} \qquad (3.15)$$

In the above equation, w_L is the system output which corresponds to tip position, and τ is the system input corresponding to joint torque at the base of the manipulator.

With the system input and output chosen, Equation 3.15 can be simplified to relate system input to system output:

$$N = B_{12}B_{44}B_{33} - B_{12}B_{34}B_{43} + B_{13}B_{34}B_{42} - B_{13}B_{44}B_{32} + B_{14}B_{43}B_{32} - B_{14}B_{33}B_{42}$$

$$w_L = - \frac{N}{B_{34}B_{42} - B_{44}B_{32}}$$

$$(3.16)$$

Where B_{ij} are elements of the overall transfer matrix in Equation 3.15. When the frequency is found which renders the function inside the brackets zero the output at that frequency will always be zero regardless of the input; therefore, the zeros of the bracketed term are the system zeros.

To search for RHP zeros, one must consider what type of frequency to input into Equation (3.16). Using the relationship which defines the Laplace variable, s

$$s = j\omega \qquad (3.17)$$

one can easily determine ω should have the form:

$$\omega = 0 - jb \qquad where \quad 0 \le b \le \infty \qquad (3.18)$$

That is, imaginary negative values of ω will result in purely real positive values of s. Thus searching Equation 3.16 with frequencies of the form of Equation 3.17 one can find the location of the RHP zeros on the real axis.

Although the location of RHP zeros is of primary concern in this research, knowledge of pole location will help in analysis of the results. Since the system damping is ignored, the poles will lie on the imaginary axis of the s-plane in complex conjugate pairs. The location of these poles can be determined by simply searching the positive imaginary axis of the s-plane. Considering the applied boundary conditions, one can extract two homogeneous equations from Equation 3.14 to get the homogeneous system:

$$\begin{Bmatrix} 0 \\ 0 \end{Bmatrix} = \begin{bmatrix} B_{32} & B_{34} \\ B_{42} & B_{44} \end{bmatrix} \begin{Bmatrix} \psi \\ V \end{Bmatrix} \qquad (3.19)$$

The poles (eigenvalues) of the system are those values of ω which make the determinant of the sub-transfer matrix in Equation 3.19 equal to zero (see reference [6] for a detailed explanation). For a two by two matrix this determinant is simply:

$$g(\omega) = B_{32}B_{44} - B_{34}B_{42} \qquad (3.20)$$

Referring to Equation 3.17, one finds that Equation 3.20 is the denominator of the input/output transfer function which is to be expected. To find the values of the purely complex poles, one must search Equation 3.20 for its roots. According to the definition of s, ω must have the form:

$$\omega = b + j0 \qquad (3.21)$$

Searching over a range of values for b will give the poles in that range. With the zero and natural frequency functions determined, the problem remains to implement a computer solution to find the RHP zeros and imaginary poles.

RESULTS

Unless otherwise specified, several dimensions remain the same from one study to the next (referred to as nominal dimensions). The overall length of the beams is 40 inches, and the height (which remains constant over length) is 1 inch. The material properties are selected to be those of aluminum: modulus of elasticity, E, is 10E6 psi, and the density is 9.55E-2 lbm/in^3.

Although the model was limited to uniform elements, there were any number of combinations one can find to represent the system. This study examined two different methods for modeling a linearly tapered beam. As shown in Figure 4.1 the link was tapered along the length in the width dimension while the height was held constant. The taper was described by two dimensions: the width at the base, A, and the width at the tip, B. The degree of taper, R=A/B, was used to compare different designs.

Using Method 1 to model the tapered link, the beam was divided into elements of equal length. For a three element model with length L, each element will have length L/3. The height of each element was the same, while the width of each element changed linearly as a function of x. Figure 4.2 presents modeling Method 1.

Using Method 2 to model the tapered link, the beam was divided into elements so the first and last element have length one-half of the intermediate elements. For a three element model with length L, the first and last elements will have length L/4 and the middle element will have length L/2. Again the height of each element was the same, while the width of each element changed linearly as a function of x. Figure 4.3 presents modeling Method 2.

Figures 4.2 and 4.3 illustrate the main difference between the two modeling methods. Method 2 compensated the elements at each end for meeting the specified end widths A and B. In both methods the width of intermediate elements was determined by the width of the tapered beam at the midpoint of each element. Since the end elements meet the specified A and B, the tapered link will not pass through the midpoint of these two elements. Method 2 compensates for this exception by making the end element lengths one half the length of the other elements.

To compare these two different modeling methods for a linearly tapered beam, a beam with nominal dimensions and A=0.75 inches and B=0.25 inches was studied. This corresponds to R=3. The number of elements was increased with each method until the zeros and poles converged. Table 4.3 presents the results from Method 1 where all elements were of equal length, and Table 4.4 presents the results from Method 2 where the end elements were half the length of all other elements. Although only two methods are considered in this research, there are many different ways to discretize a nonuniform link.

The two methods were evaluated based on an error function. When the tapered beam was modeled with 80 elements, both methods converged to nearly identical values for the poles and zeros. These values, when NE=80, were taken to be the "correct' values and other cases were compared to this case. The error, ϵ, was defined for the zeros as:

$$\epsilon = \left| \frac{z_{80,i} - z_{NE,i}}{z_{80,i}} \right| \qquad (4.2)$$

where i refers to the ith zero

A similar definition was used for the poles. The value of ϵ at the top of each column represents the maximum of all individual errors in each column. As the tables show, Method 2 provided better results for the same number of elements. In each table, one column was shaded to distinguish it as the number of elements needed to get the error under 1%. For Method 2, this column corresponded to NE=10 as opposed to NE=20 for Method 1. Thus, compensating the end elements did provide a better model of a linearly tapered beam, and this method was used in the following studies unless specified otherwise.

When comparing different link designs to evaluate pole/zero location as a function of link shape, it was

4

necessary to keep some parameter constant to aid in the evaluation. For a single-link manipulator rotating in the horizontal plane, the link's mass moment of inertia about its axis of rotation, I_y, was of importance. This parameter directly affected the dynamic equations of motion and was an important design parameter in terms of motor selection. In the following studies, several link designs were evaluated for a given value of I_y. A tapered link's moment of inertia about its axis of rotation in terms of the links parameters: L, A, B, H, and ρ is found to be:

$$I_y = \frac{\rho H}{48}(A^3 + A^2B + AB^2 + B^3 + 4AL^2 + 12BL^2)$$

$$(4.3)$$

For a given tapered link design, one can use Equation 4.3 to determine I_y. Knowing I_y, one can change the value of A and solve Equation 4.3 for B. Since the equation was cubic in B, the commercial package *Mathematica* was used to solve for B. Following this method, a group of tapered link designs were generated all with the same I_y.

The first study investigated several tapered link designs with nominal dimensions and all designs having I_y=764.05 in-lb-sec². Table 4.5 presents the raw data for each of these designs. Even with I_y held constant, it was still difficult to interpret the data. To aid in developing a relationship between zero location and link shape, the zeros were normalized with respect to the first pole for each design. The first pole is an important parameter in control system design, and normalizing the zeros with respect to the first pole aided in the interpretation of the results. Table 4.6 presents the normalized data for those designs with I_y=764.05 in-lb-sec². The second study presents data for several link designs with nominal dimensions and I_y=1528.1 in-lb-sec². Table 4.7 shows the raw data for these link designs and Table 4.8 shows the normalized data for these designs. Figures 4.4 and 4.5 show pole/zero maps for selected values of R for I_y=764.05 and I_y=1528.1 respectively.

Several patterns were evident by examining the raw data. First as a general rule, both the poles and zeros increased (moved away from the origin) as the taper on the beam increased. Increasing the taper effectively moved more of the link mass closer to the base. Increasing the value of the poles is often desirable to push them out of the system bandwidth and increase system response speed. The ordering of poles and zeros was the second pattern recognized. In a collocated system, the poles and zeros will both lie on the imaginary axis in complex conjugate pairs and in an alternating order. This means, along the imaginary axis, the poles and zero are found in the order p_1, z_1, p_2, z_2, etc. or vice versa. Previous research [18] has found this alternating order of poles and zeros does not hold for nonminimum phase systems. Referring to Table 4.5, notice the order of the magnitude of poles and zeros was: z_1, p_1, p_2, z_2, p_3, z_3, p_4, p_5, z_4.... p_2 jumped in front of z_2, and the same occurred for p_5. This reordering of poles and zeros can be critical as accurate knowledge of the pole/zero order is important for control system design.

Important information was learned from examining the relationship between the taper ratio, R, and the values of the normalized zeros. Figure 4.8 better illustrates this point showing both polynomial fits on the same graph. Even though the coefficients were different for each polynomial fit, the curves were nearly identical.

This illustrates an important relationship in the design of tapered links. For a given ratio R, the normalized zero will always remain the same. The designer can choose the location of the first pole and zero, determine the normalized zero, and then using Figure 4.8 find the appropriate taper ratio R. Of course there are constraints on this process. A ratio less than one corresponds to a taper with B greater than A, which is usually undesirable. At the other end, R is limited by the value of H. If A is larger than the value of H, the link will be wider at the base than it is tall, and the assumption that the link is stiff in the vertical plane will no longer be valid. Although the designer can choose the pole/zero relationship, the values of normalized zeros are limited to approximately 0.72-0.82 (according to Figure 4.8).

A simple verification of the above relationship is the uniform beam which has no taper. According to the stated relationship, the normalized first zero should be the same for all uniform beams. Table 4.9 presents the results for several uniform beam designs. All cases had nominal dimensions. The normalized zero in all cases was 0.726 which confirmed the normalized zero will not change as long as R is constant.

Previous studies demonstrated how the designer can choose the pole/zero relationship and then determine the appropriate taper design from the ZERO results. This study presents the designer with another freedom. Once the taper is chosen, the designer can change the link to independently adjust the value of I_y. Table 4.10 presents the results of a study performed on designs with L=40 inches, and all designs have the same taper. The height of the link was changed to adjust the value of I_y.

One should notice that the pole and zero locations of all designs in Table 4.10 were the same, yet the value of I_y changed with adjustments in link height. Since the adjustment of H is out of the plane of motion, it had no effect on the location of poles and zeros. Combining this with the results from the previous study, the designer can effectively choose the location of poles and zeros and independently adjust the links moment of inertia about its axis of rotation to meet the needs of the particular system.

CONCLUSIONS

Program ZERO was developed as a tool to locate the poles and zeros of a single-link manipulator modeled as a pinned-free Euler-Bernoulli beam. The program used transfer matrix theory to allow for variable cross-sections granting the designer new freedom in analysis of nonuniform link designs. The results were shown to be very accurate when system pole location was compared to analytic solutions for uniform beams. Several results from previous studies were confirmed with this research.

First, the reordering of poles and zeros was confirmed for nonminimum phase systems. Accurate knowledge of pole/zero order is critical for proper control system design. In conjunction with this, Tables 4.3 and 4.4 show that even for very few elements in the model, the program still predicts the proper order of poles and zeros.

Second, the studies presented suggested the nonminimum phase characteristics could not be eliminated by changing the structural design of the link. The system will be nonminimum phase above a finite frequency dictated by the location of the first nonminimum phase zero. It may be possible that this frequency is out of the operating range and not of concern to the designer.

The major contributions of this research are the development of the ZERO program to determine zero and pole location for a single-link nonuniform flexible manipulator, and formulation of a design procedure to place the first pole and zero and independently change the value of the link's moment of inertia about its axis of rotation to meet the needs of the system.

Program ZERO was set up specifically for pinned-free boundary conditions of the model and determines pole and zero location based on a frequency range entered by the user. Linearly tapered beams were studied in this research, but any type of nonuniform beam can be analyzed by program ZERO. Slight modifications would also allow for different boundary conditions.

The design procedure for tapered beams allows the designer to choose the first pole and zero subject to certain physical constraints. These physical constraints only allow for approximately 25% variation in R according to Table 4.6. This zero to pole ratio defines a particular taper ratio according to the collected data. Keeping the ratio the same, the size of the taper can be changed to get the proper magnitude of the pole and zero. With the pole and zero placed, the height of the beam can be changed to adjust the link's moment of inertia about its axis of rotation. This procedure can be used to design tapered links to meet the particular requirements of the system.

Program ZERO was designed to model a single-link manipulator modeled with pinned-free boundary conditions. This is a simplified model, but it was necessary to show transfer matrices yield good results for this case before progressing to more complicated problems. Now that transfer matrices have proven useful to solve for zero location, future work exists to extend the results of this research.

First, the program could be modified so the user could input the desired boundary conditions which best represent the system. This could include hub inertia or end-point mass. Second, the program could be extended to multi-link designs to predict pole and zero location for different configurations. Transfer matrices have been derived for rotary joints and many other elements. The DSAP package developed by Book, et. al. [6] handles multi-link models and would be a good reference. Finally, the results for tapered link designs could be applied to the inverse dynamic algorithm developed by Kwon and Book [9]. This method requires mode shapes for the assumed modes and uses pinned-pinned boundary conditions, which can also be found using transfer matrix techniques as shown in Book, et al.[6].

ACKNOWLEDGEMENTS

BIBLIOGRAPHY

[1] Asada, H., Park, J.-H., and Rai, S., "A Control-Configured Flexible Arm: Integrated Structure/Control Design," *Proceedings of the 1991 IEEE International Conference on Robotics and Automation*, Sacramento, California, April, 1991, pp. 2356-2362.

[2] Bayo, E., "A Finite Element Approach to Control the End-Point Motion of a Single-Link Flexible Robot," *Journal of Robotic Systems*, Vol. 4, No. 1, 1987, pp.63-75.

[3] Beer, Ferdinand, and Johnson, Russell, Jr., *Vector Mechanics for Engineers, Statics and Dynamics*, Third Edition, McGraw-Hill, New York, 1977.

[4] Book, W. J., *Design and Control of Flexible Manipulator Arms*, Ph.D. Thesis, Massachusetts Institute of Technology, April, 1974.

[5] Book, W. J., and Kwon, D.-S., "Contact Control for Advanced Applications of Light Weight Arms," *Symposium on Control of Robots and Manufacturing*, Arlington, Texas, 1990.

[6] Book, W. J., Majette, M., and Ma, K., *The Distributed Systems Analysis Package (DSAP) and Its Application to Modeling Flexible Manipulators*, NASA Contract NAS 9-13809, Subcontract No. 551, School of Mechanical Engineering, Georgia Institute of Technology, 1979.

[7] Churchill, R. V., and Brown, J. W., *Complex Variables and Applications*, Fifth Edition, McGraw-Hill Publishing Company, New York, 1990.

[8] Kwon, D.-S., *An Inverse Dynamic Tracking Control for Bracing A Flexible Manipulator*, Ph.D. Dissertation, Georgia Tech, Woodruff School of Mechanical Engineering, June, 1991.

[9] Kwon, D.-S., and Book, W. J., "An Inverse Dynamics Method Yielding Flexible Manipulator State Trajectories," *Proceedings of the American Control Conference*, June, 1990, pp. 186-193.

[10] Majette, M., *Modal State Variable Control of a Linear Distributed Mechanical System Modeled with the Transfer Matrix Method*, Master's Thesis, Georgia Tech, Woodruff School of Mechanical Engineering, June, 1985.

[11] Meirovitch, L., *Elements of Vibrational Analysis*, McGraw-Hill, New York, 1986.

[12]   Misra, Pradee, "On The Control of Non-Minimum Phase Systems," *Proceedings of the 1989 American Control Conference*, 1989, pp. 1295-1296.

[13]   Nebot, E. M., Lee, G. K. F., and Brubaker, T. A., "Experiments on a Single Link Flexible Manipulator,", *Proceedings from the USA-Japan Symposium on Flexible Automation Crossing Bridges: Advances in Flexible Automation and Rob s*, 1988, pp. 391-398.

[14]   Park, J.-H., and Asada, H., "Design and Analysis of Flexible Arms for Minimum-Phase Endpoint Control," *Proceedings of the American Control Conference*, 1990, pp. 1220-1225.

[15]   Park, J.-H., and Asada, H., "Design and Control of Minimum-Phase Flexible Arms with Torque Transmission Mechanisms," *Proceedings of the 1990 IEEE International Conference on Robotics and Automation*, 1990, pp. 1790-1795.

[16]   Pestel and Leckie, *Matrix Methods in Elastomechanics*, McGraw-Hill, New York, 1963.

[17]   Rao, Singiresu S., *Mechanical Vibrations*, Addison-Wesley Publishing Company, Reading, Massachusetts, 1986.

[18]   Spector, V. A., and Flashner, H., "Modeling and Design Implications of Noncollocated Control in Flexible Systems," *Journal of Dynamic Systems, Measurement, and Control*, Vol. 112, June, 1990, pp. 186-193.

[19]   Spector, V. A., and Flashner, H., "Sensitivity of Structural Models for Noncollocated Control Systems," *Journal of Dynamic Systems, Measurement, and Control*, Vol. 111, December, 1989, pp. 646-655.
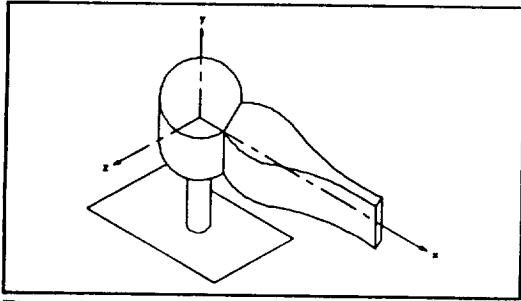
Figure 3.1: Single-Link, Flexible Manipulator
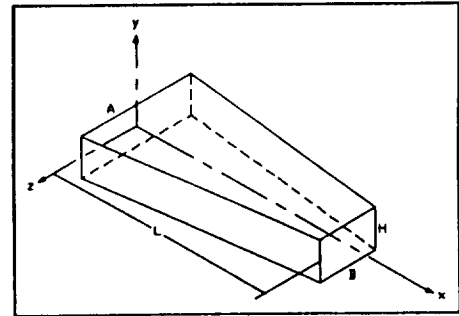
Figure 4.1: Tapered Link Diagram
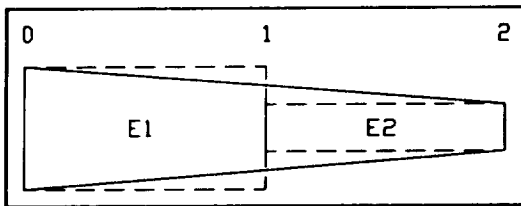
Figure 3.3: Simple Model of a Tapered Beam
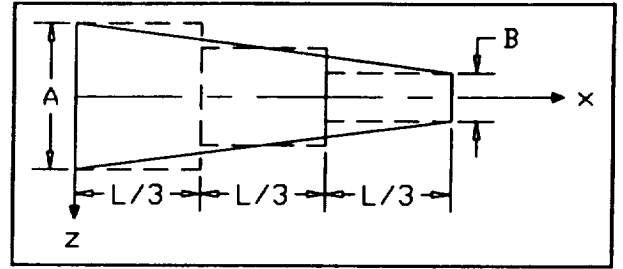

Figure 4.2: Modeling Method 1
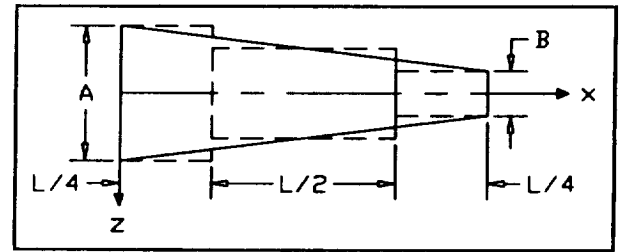
Figure 4.3: Modeling Method 2
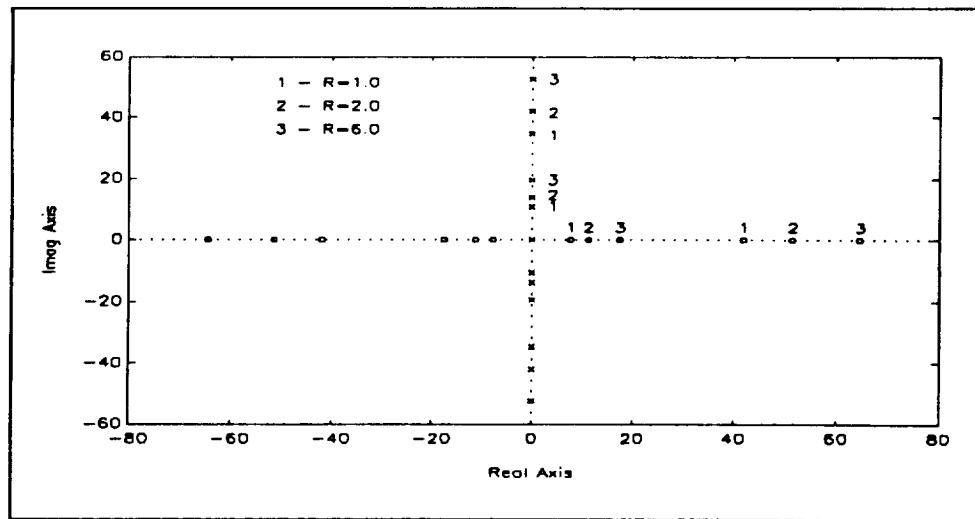
Figure 4.4: Pole/Zero Map of Selected Designs For $I_y = 764.05$

8

100

1 — R—1.0
2 — R—1.5
3 — R—2.0

50

Imag Axis

0

−50

−100

−150   −100   −50   0   50   100   150

Real Axis
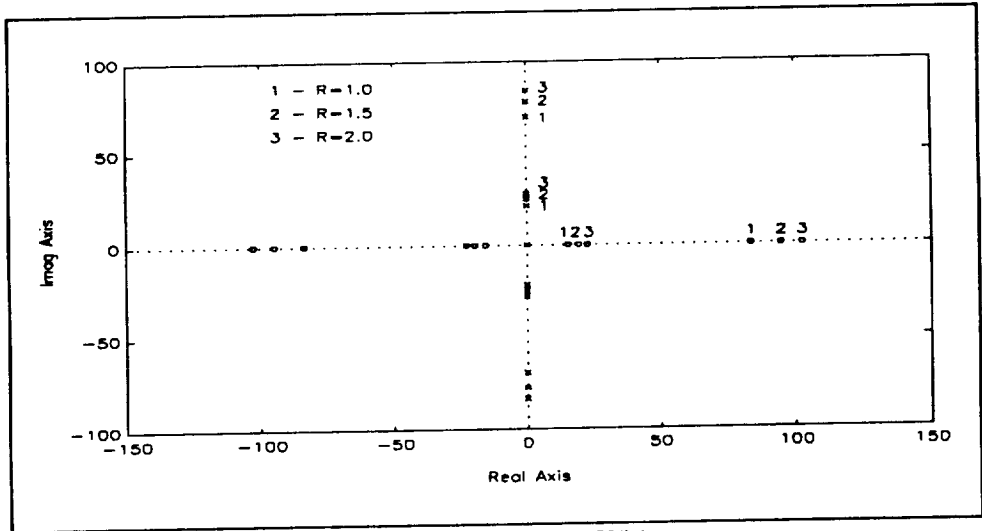
Figure 4.5: Pole/Zero Map of Selected Designs For I_y=1528.1

0.82

0.8

Normalized Zero

0.78

0.76

0.74

0.72

1   1.1   1.2   1.3   1.4   1.5   1.6   1.7   1.8   1.9   2

R

− − Iy=764.05

−−− Iy=1528.1
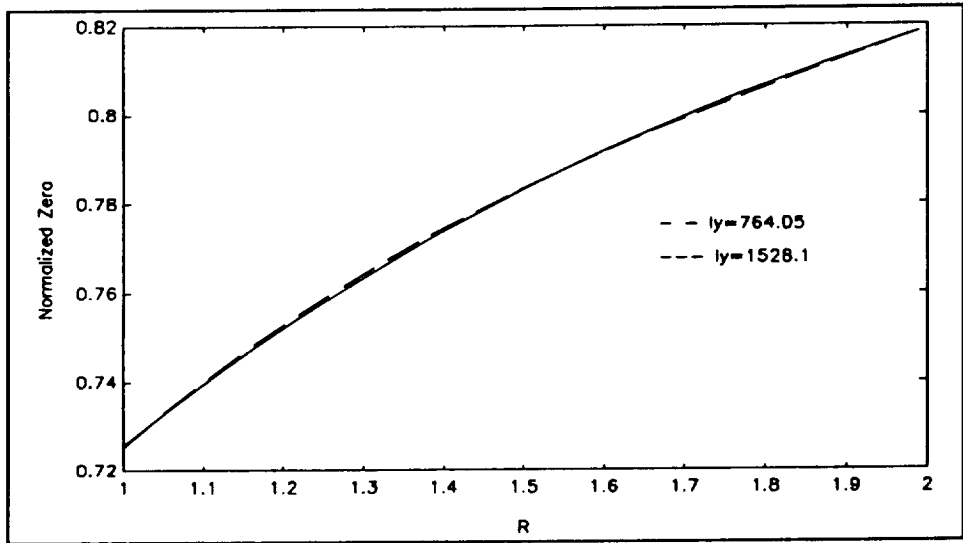
Figure 4.8: Comparison of Polynomial Curve Fits

Table 4.3: Results From Method 1

| Zero Pole	NE=3 (ε≤20%)	NE=5 (ε≤8.6%)	NE=10 (ε≤1.9%)	NE=20 (ε≤0.3%)	NE=40 (ε≤0.1%)	NE=80
1	13.91 13.64	13.99 15.95	13.73 16.05	13.69 15.96	13.68 15.92	13.68 15.91
2	45.57 38.08	55.99 43.24	57.28 46.19	56.91 46.21	56.84 46.14	56.83 46.11
3	121.2 88.16	122.0 85.31	134.2 92.52	133.8 93.20	133.6 93.13	133.5 93.09
4	210.8 137.5	223.2 147.5	242.9 154.9	244.7 157.0	244.2 157.0	244.1 157.0
5	357.8 219.5	383.8 234.7	382.1 233.3	389.4 237.7	388.9 237.9	388.7 237.8

Table 4.4: Results From Method 2

Zero Pole	NE=3 (ε≤16%)	NE=5 (ε≤4.0%)	NE=10 (ε≤0.4%)	NE=20 (ε≤0.1%)	NE=40 (ε≤0.0%)	NE=80
1	13.09 15.57	13.49 15.82	13.64 15.89	13.67 15.90	13.68 15.91	13.68 15.91
2	53.77 38.66	56.12 45.82	56.62 46.03	56.78 46.09	56.82 46.10	56.83 46.10
3	120.4 85.88	135.1 93.17	133.0 92.90	133.4 93.03	133.5 93.06	133.5 93.06
4	233.6 154.4	234.7 148.3	243.4 156.6	243.9 156.9	244.1 156.9	244.1 156.9
5	360.6 220.3	384.6 231.1	388.2 237.4	388.3 237.7	388.6 237.7	388.6 237.8

Table 4.5: Tapered Beams With I_y=764.05

Zero Pole	A=.375 B=.375	A=.4 B=.367	A=.5 B=.333	A=.6 B=.3	A=.7 B=.267	A=.8 B=.233	A=.9 B=.2	A=1 B=.167
1	7.745 10.68	8.153 11.04	9.762 12.46	11.34 13.84	12.90 15.21	14.44 16.60	15.98 18.03	17.50 19.52
2	41.85 34.59	43.15 35.48	47.38 38.80	51.37 41.87	55.05 44.73	58.45 47.41	61.60 49.94	64.51 52.36
3	103.4 72.18	105.9 73.88	115.0 80.17	123.1 85.75	130.2 90.75	136.4 95.19	141.7 99.14	146.2 102.6
4	192.2 123.4	196.6 126.2	212.7 136.5	226.6 145.5	238.6 153.4	248.7 160.1	257.1 165.9	263.6 170.6
5	308.4 188.3	315.3 192.6	340.5 208.0	362.0 221.2	380.3 232.6	395.5 242.3	407.8 250.3	416.9 256.5

Table 4.6: Normalized Data For I_y=764.05

Zero	R=1.00	R=1.09	R=1.50	R=2.00	R=2.62	R=3.43	R=4.50	R=5.99
1	0.7252	0.7385	0.7835	0.8194	0.8481	0.8699	0.8863	0.8965
2	3.919	3.909	3.803	3.712	3.619	3.521	3.417	3.305
3	9.682	9.592	9.230	8.895	8.560	8.217	7.859	7.490
4	18.00	17.81	17.07	16.37	15.69	14.98	14.26	13.50
5	28.88	28.56	27.33	26.16	25.00	23.83	22.62	21.36

Table 4.7: Tapered Beams With I_y=1528.1

Zero Pole	A=.75 B=.75	A=.8 B=.733	A=.9 B=.7	A=1.0 B=.667	A=1.1 B=.633	A=1.2 B=.600
1	15.49 21.35	16.31 22.08	17.92 23.51	19.52 24.92	21.11 26.30	22.68 27.68
2	83.71 69.16	86.03 70.95	90.50 74.35	94.76 77.60	98.83 80.73	102.7 83.74
3	206.7 144.4	211.7 147.7	221.2 154.2	230.1 160.3	238.4 166.1	246.2 171.5
4	384.4 246.8	393.2 252.5	409.9 263.1	425.4 273.1	439.9 282.4	453.2 291.0
5	616.7 376.7	630.6 385.1	656.8 401.1	681.0 415.9	703.3 429.6	724.0 442.4

Table 4.9: ZERO Results For Uniform Beam Designs

Zero Pole	W=0.25"	W=0.5"	W=0.75"
1	5.163 7.116	10.33 14.23	15.49 21.35
NZ	0.726	0.726	0.726
2	27.90 23.06	55.80 46.12	83.71 69.19
3	68.90 48.12	137.8 96.23	206.7 144.3
4	128.1 82.28	256.2 164.6	384.4 246.8
5	205.6 125.6	411.1 251.1	616.7 376.7

Table 4.10: Variable Height Designs

Zero Pole	H=1.0"	H=1.5"	H=2.0"
1	11.34 13.84	11.34 13.84	11.34 13.84
2	51.37 41.87	51.37 41.87	51.37 41.87
3	123.1 85.75	123.1 85.75	123.1 85.75
4	226.6 145.5	226.6 145.5	226.6 145.5
5	362.0 221.2	362.0 221.2	362.0 221.2
I_y	764.05	1146.1	1528.1